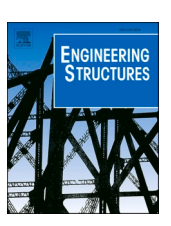
ELSEVIER

Contents lists available at ScienceDirect

Engineering Structures

journal homepage: www.elsevier.com/locate/engstruct





Effect of partition walls on the seismic response of mass-timber buildings with a post-tensioned rocking wall system

Hamed Hasani *, Keri L. Ryan

Department of Civil and Environmental Engineering, University of Nevada-Reno, Reno, NV, United States

ARTICLE INFO

Keywords:
Partition walls
Seismic response
Mass-timber buildings
Post-tensioned rocking wall
Nonstructural components
Structure-nonstructural interaction
Low damage partitions
Numerical modeling

ABSTRACT

The structural-nonstructural interaction effects of nonstructural partition walls and post-tensioned CLT rocking walls in mass-timber buildings were evaluated in a parametric study. Representative 2D rocking wall units in 5-story and 12-story mass-timber archetype buildings were modeled in OpenSees. Moreover, concentrated spring models were developed to represent effective force-deformation for four different variations of partition wall detailing, and applied to the building models to represent wall densities associated with apartment and hospitality occupancies. Eigenvalue, pushover, and response-history analyses were performed on 2D models of the bare structure and those with partition wall variations. Including partition walls with fixed connection details was found to decrease story drifts and rocking wall story shears compared to the bare frame model by up to 50% in a service earthquake and up to 30% in a maximum considered earthquake. However, partition walls with deformation-compatible details were found to have negligible influence (less than 5%) on the response.

1. Introduction

Recent advancements in structural engineering have led to new structural systems that can reduce earthquake-induced damage and promote seismic resilient responses. However, damage to nonstructural elements has led to considerable economic losses in recent earthquakes [33,12,45,24,26,16,14]. Such elements are susceptible to damage that leads to considerable downtime at low shaking intensity, and also comprise the majority of construction cost [39]. Therefore, to achieve a resilient structure, the resilience of both structural and nonstructural components is essential.

Partition walls are one of the most common nonstructural components within a building. Connected floor-to-floor, they are subjected to the differential displacement demands or inter-story drifts, which vary throughout the building. Partition walls are prone to initial damage at inter-story drifts as low as 0.1% [25]. Partition walls are usually not anticipated to contribute to the primary load-bearing or lateral load resisting system; and their stiffness, strength and location are not accounted for in the design. However, previous research has shown that accounting for the stiffness and strength of partition walls can influence the dynamic characteristics and seismic response of the structure. A few experimental studies examined the contribution of partition walls in the

seismic response of structures. For example, Lee et al. [18] and Tasligedik et al. [40] performed quasi-static testing of partition walls built as infill walls within a moment frame, and showed that the strength of partition walls is not negligible compared to the frame alone. In addition, some studies evaluated the effect of partition walls on the dynamic behavior of structural subassemblies or buildings during shake table testing [13,19,20,22,38,44]. Finally, the seismic effect of partition walls was evaluated in numerical studies as well. For example, partition walls were shown to decrease the fundamental period up to 14% in a hospital building with a steel moment frame [47]. The detailing of the partition wall connections influences their contribution to the system response. Another numerical study showed that traditionally detailed steel or timber framed partition walls led to a 10% reduction in the period of a 10-story reinforced concrete building, while alternative low damage details had no influence on the system period [41]. A variety of alternative drift-compatible details intended to reduce seismic damage in partition walls are being developed; observed hysteresis loops show that walls with alternative detailing have lower stiffness and strength than conventional partition walls [42,28,1,27;17;36].

With regard to structural resilience, self-centering systems have emerged as a promising class of lateral systems for advanced seismic protection, but such systems are flexible and may have more significant

E-mail address: hasani@nevada.unr.edu (H. Hasani).

^{*} Corresponding author at: Department of Civil and Environmental Engineering, University of Nevada, Reno/MS 0258, 1664 N. Virginia Street, Reno, NV 89557, United States.

drift than conventional systems due to reduced hysteretic damping [5]. For example, buildings with post-tensioned reinforced concrete rocking walls were shown to have longer periods and larger inter-story drifts than buildings with traditional reinforced concrete walls [48]. Posttensioned rocking walls built from mass timber components, such as cross-laminated timber (CLT) panels, have been developed as a lateral system for mass timber buildings. Combining a flexible post-tensioned rocking wall system and the inherent flexibility of timber compared to concrete can result in a building with considerable flexibility. Previous studies have shown the potential for post-tensioned CLT rocking walls as a resilient lateral load resistant system for tall buildings in high seismic areas, as they can develop and sustain large drift demands with minor damage [4,8,15,23,30,31,32]. Furthermore, since mass timber buildings with post-tensioned CLT rocking walls are pretty flexible, the stiffness contribution of different partition walls might significantly affect the seismic response of these types of buildings.

For mass timber buildings with post-tensioned CLT rocking walls, this research aims to 1) understand how the partition wall detailing affects the structure-nonstructural interaction, such as dynamic properties of the structural system, and 2) determine whether these nonstructural walls should be considered part of the overall building resistance and accounted for in the design. For this purpose, different partition wall models were applied within models of 2D CLT rocking wall units to represent the response of mass timber archetype buildings. Finally, the seismic response of the bare structure and combined models were evaluated to determine the effect of different partition walls on the overall system response.

2. Modeling of partition walls

2.1. Partition wall details

Interior partition walls are framed with horizontal tracks at the top and bottom and vertical studs connected to the tracks, then covered with drywall (Fig. 1(a)). The framing can be timber or steel; however, steel framing is more common than timber framing in modern buildings due to its higher ductility [40]. Therefore, steel-framed partition walls are considered in this study.

Many construction details can affect the performance of partition walls, but the details of connecting the partition walls to the structural system have the most effect on their seismic response [28]. In general, there are two approaches for connecting partition walls to the surrounding structural elements: "fixed" and "slip-track" connections. In fixed detailing, the studs and drywall are connected to tracks on top and bottom (Fig. 2(a)). In slip-track detailing, the partition walls are isolated from the inter-story drift by eliminating the connection of studs and drywall to the top track (Fig. 2(b)). Walls with fixed connections are observed to generally have higher stiffness and strength than those with slip-track connections [7,6,47]. However, basic slip-track detailing leads to damage at the intersection with the adjacent out-of-plane or return wall, as the slip of the in-plane wall causes it to collide with the return wall (Fig. 1(b)-(c)). For slip-track detailed walls, this interaction with return walls increases the stiffness and strength relative to those with no

return walls. In addition, details under development to reduce damage at return walls, as mentioned earlier, are expected to have lower stiffness and strength.

The seismic response of interior partition walls with fixed connections and slip track connections (with and without return walls) was characterized during a series of tests at the University at Buffalo [7,6] (Fig. 3(a)). The partition wall specimens were 3.6 m long by 3.5 m high (main in-plane wall dimension), built from lightweight steel framing, and used institutional construction details (0.75 mm minimum framing thickness, 406 mm minimum stud spacing, and extra reinforcement through the corners [34]. Moreover, in slip-track detailing, studs and gypsum were connected to the bottom track. Recorded responses of specimens from this program were used to develop numerical models of the wall response for various details [47]. Select models from this study have been adapted here to represent the general response of fixed and slip track connections when return walls are present. More details can be found in Wood and Hutchinson [47].

In addition, two other wall configurations with innovative details intended to reduce the drift-induced damage at the intersecting partition walls are considered in this study. The numerical responses of these walls were generated in an experimental test of C-shaped walls performed at Natural Hazards Engineering Research Infrastructure (NHERI) Lehigh Equipment Facility in 2019 (Fig. 3(b)). The main in-plane walls were 3.8 m long by 3.5 m high, and built with an institutional-grade construction (0.88 mm thickness framing and 406 mm stud spacing) and slip-track detailing. The first distributed gap (DG) detail incorporated frequent expansion joints through the length of the wall (Fig. 2 (c)), while the second corner gap (CG) detail incorporated a full gap through the intersection of the wall (Fig. 2 (d)). Although the DG and CG walls were subjected to a bi-directional quasi-static reversed cyclic test, the models developed for this study were based on the in-plane response. More details can be found in Hasani and Ryan [17].

Fig. 4 presents the backbone curve force versus displacement of walls with each of the four considered details, which are used in the numerical models. The fixed connection detail offers more than twice the resistance of any of the other details, while novel details have lower resistance than traditional slip track detail. Specifically, the CG detailing generates almost no resistance, and its response is similar to the sliptrack detailing without return walls. Full experimental hysteresis loops for each detail can be found in Wood and Hutchinson [47] and Hasani and Ryan [17].

2.2. Partition wall modeling

To date, two classes of models have been developed for predicting partition wall cyclic response. In the first or finite element approach, all components and connections of partition walls are represented by separate elements. This approach is used to study the effect of specific details and configurations of partition walls and develop the fragility curves (e.g. Rahmanishamsi et al. [35]). In the second or simplified approach, concentrated spring elements represent the total partition wall response, and the global hysteretic force-deformation response of the designated length of the partition wall is assigned to a single spring.

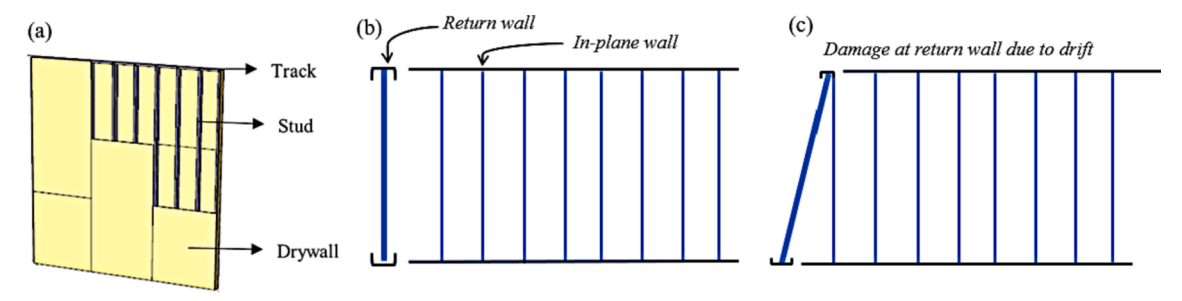


Fig. 1. (a) Partition wall components; and for wall with slip track detailing (b) original configuration and (c) movement under in-plane drift.

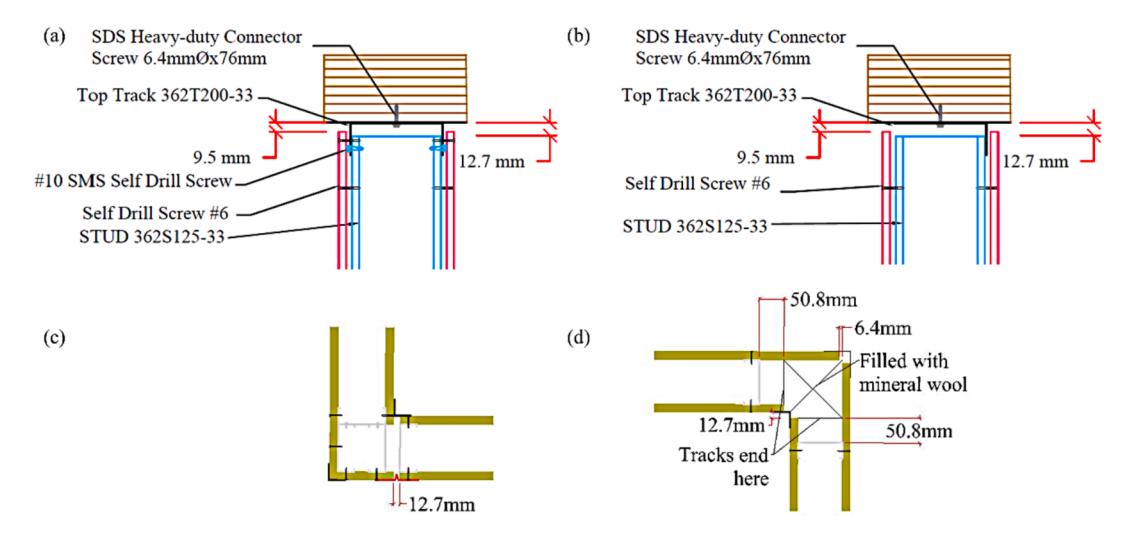


Fig. 2. (a) Fixed connection detailing, (c) slip track detailing, (c) distributed gap detail corner expansion joint, (d) corner gap detail.

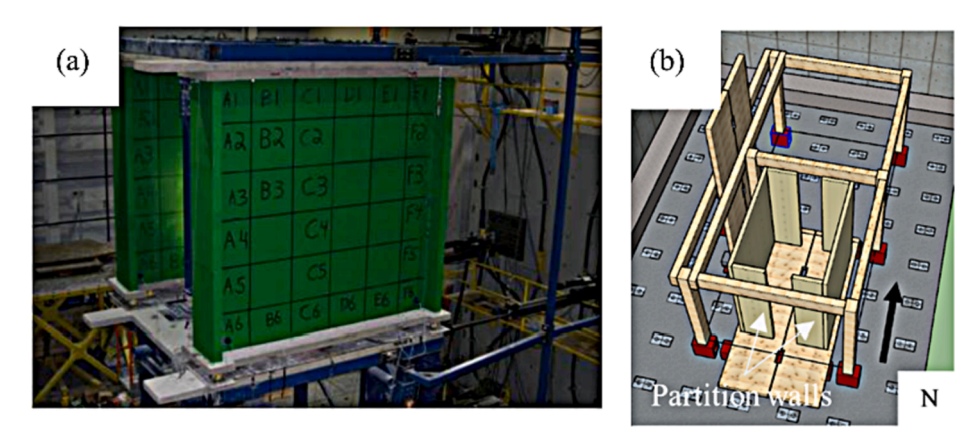


Fig. 3. (a) Experimental test at University at Buffalo [6,7], (b) Experimental test at NHERI@Lehigh [17].

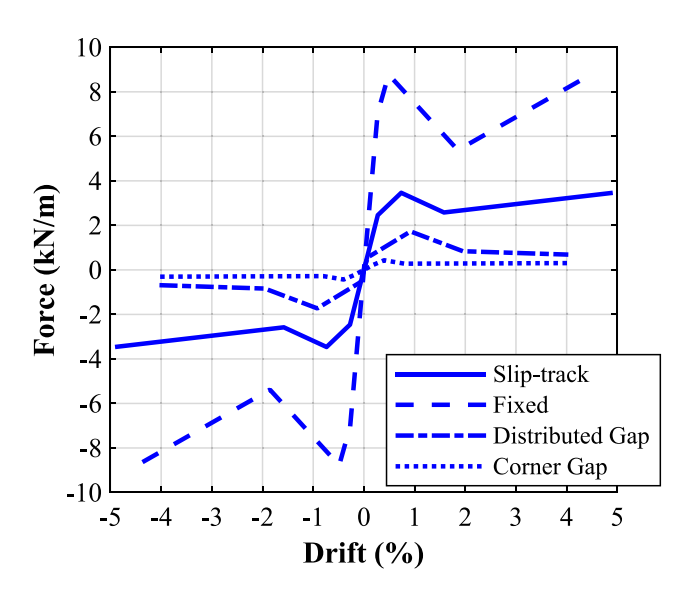


Fig. 4. (a) Backbone curves of different partition walls.

The simplified approach is helpful in high-level building simulations incorporating structure-nonstructural interaction (e.g. [7,6,19,37,41,47]). In addition, this approach facilitates implementing numerous partition walls within a building while maintaining a fast and

efficient analysis.

Due to the aims of this research, the simplified approach was used for modeling the nonlinear hysteretic response of partition walls, and the models were generated in OpenSees [21]. In general, the hysteretic response of this class of partition walls is characterized by a pinching force-displacement cyclic behavior, where each cycle shows degradation in strength and stiffness compared to the previous cycle. Therefore, the available pinching material in OpenSees (Fig. 5) was used to model partition walls by calibrating the material model to various experimentally observed force-deformation backbone curves. The calibrated hysteretic response of each wall is shown in Fig. 6; note that the force axes are different scale and thus the slip track details (especially distributed gap in Fig. 6(c) and corner gap in Fig. 6(d)) have significantly lower resistance than the fixed connection detail (Fig. 6(b)). These models have been normalized by wall length; thus, the force is multiplied by the wall length for application in a building model.

3. Development of the structural model

Next, 5-story and 12-story archetype buildings with post-tensioned CLT rocking wall lateral systems were modeled to evaluate the influence of various partition walls on their overall seismic response. These hypothetical buildings, designed by Wilson [46], are designed for lateral resistance provided by the CLT rocking walls.

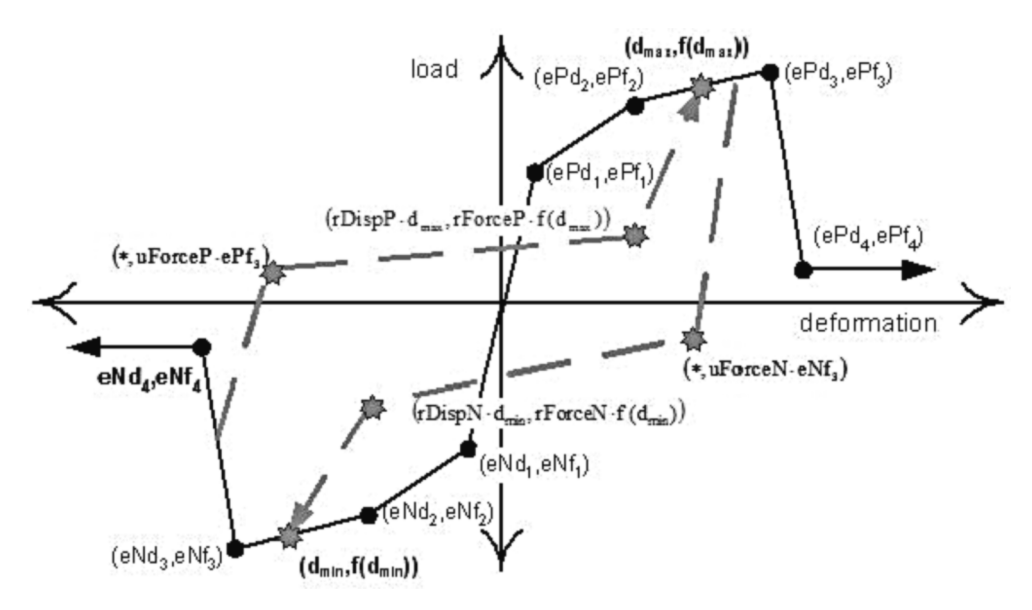


Fig. 5. Pinching material [21].

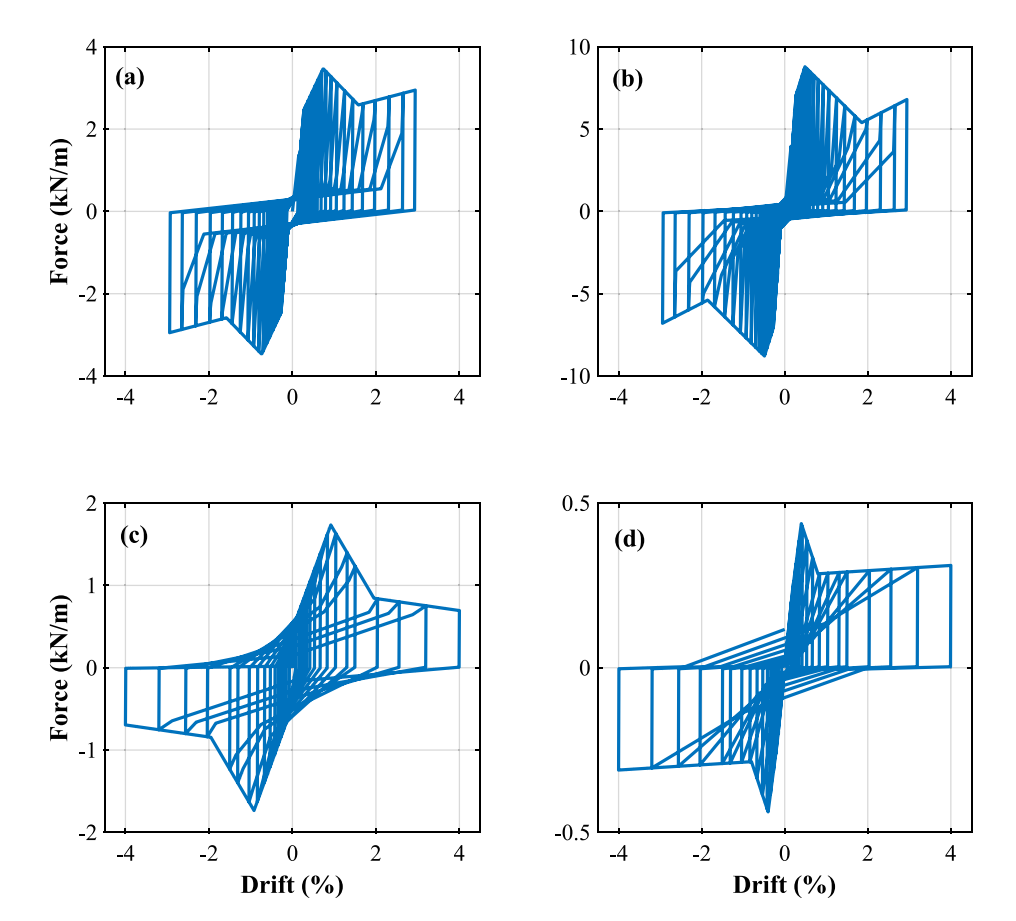


Fig. 6. Hysteresis loops using calibrated models of partition walls (a) Slip-Track (b) Fixed (c) Distributed Gap (d) Corner Gap.

3.1. Building design specifications

Fig. 7 depicts the buildings that were modeled in this research. The 5-story building, shown in Fig. 7(a), is 19.81 m tall with 3.96 m story heights and floor dimensions of 27.5 m by 51.1 m. The 12-story building (Fig. 7(b)) measures 45.72 m tall with story heights of 3.81 m, and floor dimensions of 27 m by 74.25 m. Post-tensioned CLT rocking walls are distributed throughout both buildings in both directions, as shown in

Fig. 8. These buildings were designed for the South Lake Union neighborhood of Seattle (coordinate: 47.6222° N, -122.3346° W), risk category II, and site class D [46].

The five-story building has 6 and 4 coupled rocking wall units in the N-S and E-W direction, respectively, while the 12-story building has eight coupled rocking wall units in each direction. Each coupled rocking wall unit consists of three adjacent post-tensioned wall panels coupled with U-shaped flexural plates (UFP) for energy dissipation. A conceptual

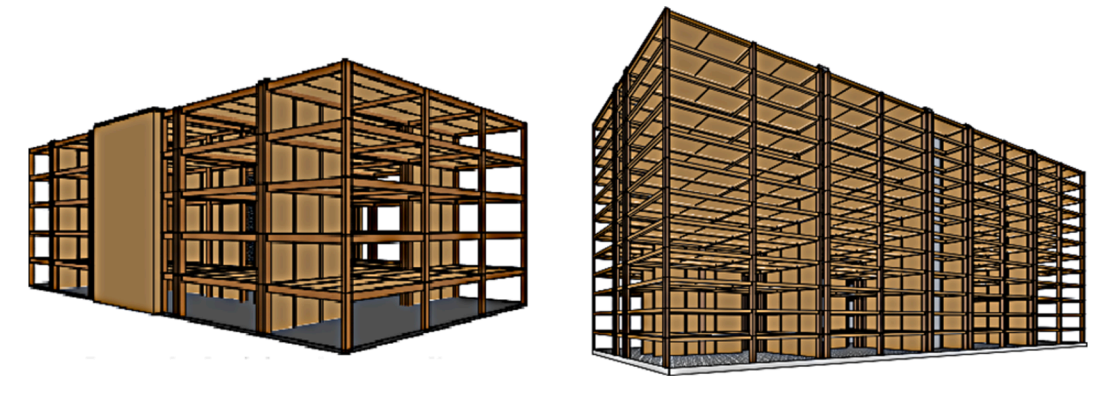


Fig. 7. (a) 5 story building (b) 12 story building [46].

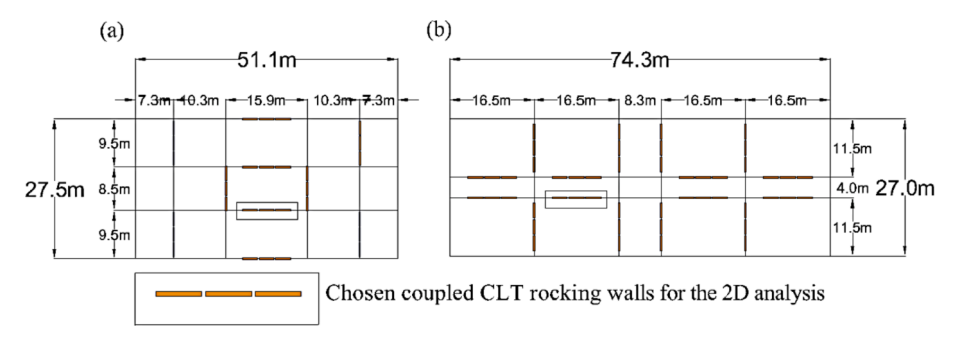


Fig. 8. Prototype building plans showing CLT coupled rocking walls. (a) 5-story (b) 12-story building.

illustration of coupled rocking walls with post-tensioning and UFPs is shown in Fig. 9. The rocking wall panels are 9-ply (315 mm thick) CLT panels, 3.05 m in length, except for the 5-story in N-S direction, for which the panels are 2.75 m in length. Two UFPs connect each adjacent set of panels on each floor, with a total of 4 UFPs per floor per coupled wall unit. Each UFP uses steel with yielding strength of 413 MPa and has width of 30 cm, thickness of 1.25 cm, and inner diameter of 10 cm, respectively. Post-tensioning (PT) rods extend from the tops of the walls down to the foundation in each building; each wall panel is post-

tensioned with four bars with a total area of 6193 mm² centered on the wall panel (both buildings), and initial PT forces of 530 kN and 1800 kN per wall panel in the 5-story and 12-story, respectively. Shear is transferred at the base of the rocking wall through friction.

The coupled rocking walls are connected to the gravity framing with slotted pin connections. Thus, the rocking walls are isolated from the gravity loading of the rest of the building and carry only their self-weight. Some of the material properties of buildings can be found in Table 1. More information can be found in Wilson [46].

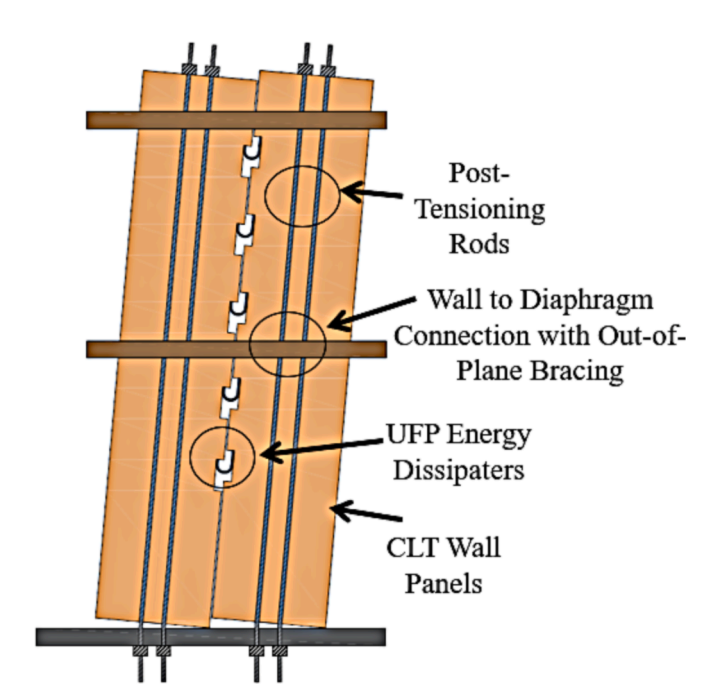


Fig. 9. Components of coupled post-tensioned rocking wall system.

3.2. Structure model

Two-dimensional (2D) models of a single coupled rocking wall unit with the standard 3 m wall panel length were developed in OpenSees for each building (Fig. 10). One-fourth and one-eighth of the mass of the buildings were assigned to each model for the 5-story and 12-story, respectively. The models consisted of a few main components, including elastic Timoshenko beam-columns for wall panels, multispring contact elements for base rocking, truss elements for PT bars, and zero-length spring elements for UFPs.

The wall panels were modeled using a series of elastic Timoshenko beam-column elements spanning between UFP and floor locations. The nonlinear rocking behavior of the panels and the compressive deformation of the CLT were modeled using multi-spring contacts at the base of each panel. The contact stiffness was calculated using the following equation:

Table 1Material properties of structural components.

Material	CLT	•		PT (rods)	UFP		
Property	E (MPa)	G (MPa)	f _y (MPa)	E (MPa)	f _y (MPa)	f _u (MPa)	f_y (MPa)
Value	4215	219	37	200,000	882	1034	413

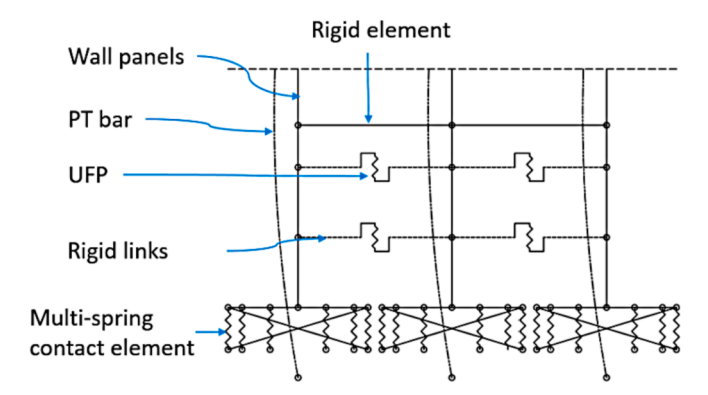


Fig. 10. Two-dimensional (2D) models of the first story of a coupled rocking wall unit.

$$K_{s} = \frac{AE}{L_{p}} \tag{1}$$

where A and E are the cross-sectional area and elastic modulus of the CLT panels, and L_p is the plastic hinge length of the wall. The assumed plastic hinge length was 254 mm, which resulted in a stiffness of 2.0e8 kN/m. This stiffness was distributed – according to Gauss-Lobatto rules – to 80 zero-length springs for each wall panel. The compression response and gap opening of the zero-length springs were modelled by a compression-only elastic, perfectly plastic gap material (ElasticPPGap in OpenSees). Finally, corotational truss elements were applied to transfer shear at the base of rocking walls.

The PT bars were modeled using tension-only corotatonal truss elements with a bi-linear hysteretic material model. These elements were fixed at the base and connected to the top panel beam-column element at the roof. An initial strain was applied to these truss elements using an the InitStrainMaterial in OpenSees, combined with a MinMax material to track the ultimate strain of the PT bars. For the UFPs, a uniaxial Giuffre-Menegotto-Pinto steel material model with isotropic strain hardening was assigned to zero-length spring elements. Based on Baird et al. [3], the effective yield force, initial stiffness, and R factor for the UFPs were determined to be 91.63 kN, 20,577 kN/m, and 14.7, respectively. R is a unitless parameter that determines the transition from elastic to postyield region of the force-displacement curve. Rigid elements were used to link the elastic beam-column wall elements at the center of the panels to the zero-length UFP springs located between the two wall panels. The main dimensions of UFPs and calculated specifications for the material models can be found in Table 2. The adjacent rocking wall panels were connected by rigid links (very stiff truss elements) at the floor levels that represented the diaphragms.

4. Coupled structure-partition wall model

The concentrated spring elements representing the resistance of the partition walls were added to the 2D wall unit model, as shown in Fig. 11. As discussed previously, partition wall resistance was represented by translational spring elements, and the nonlinear hysteretic force-displacement relations of different partition walls (Fig. 6) were assigned to these translational springs. The spring elements were connected to nodes at mid-height that were slaved to structural nodes at the top and bottom of the story in all degrees of freedom. As a result, the partition wall hysteretic responses were lumped at the story mid-height.

Partition wall indices were used to determine representative wall

Table 2 UFP specifications.

Dimensions	b _u (mm)	D_u (mm)	t _u (mm)	F_y (kN)	K_0 (kN/m)	R
Value	279	102	12.7	91.63	20,577	14.7

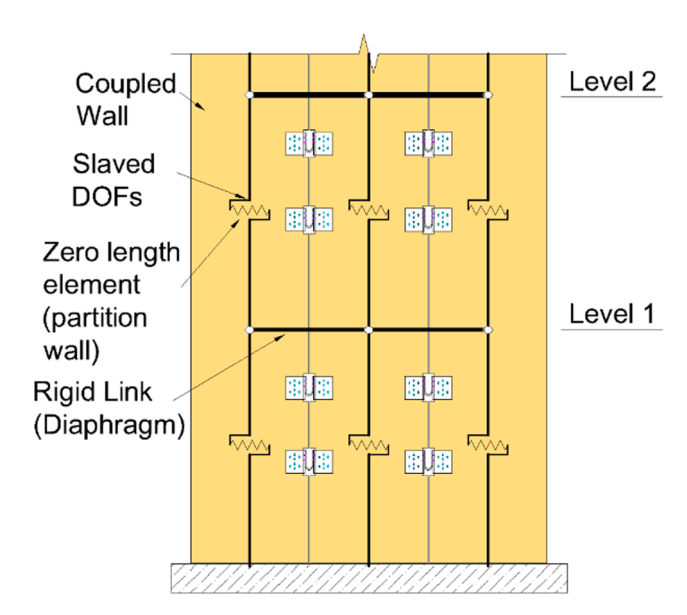


Fig. 11. Partition wall implementation into lateral load resisting system.

length in the building. The partition wall index is defined as the total length L of partition walls per story divided by the plan area A of the floor (with units 1/Length). Two partition wall indices were chosen from eight available occupancies in the FEMA P-58, Normative Quantity Estimation Tool FEMA [11]. Apartment occupancy represents an upper bound partition wall density, with a partition wall index of 0.12. Hospitality occupancy represents an average partition wall density, with a partition wall index of 0.06. Since partition walls run in both directions, one-half of the density was applied to the 2D models. Table 3 tabulates the calculated total partition wall lengths and the partition wall length assigned to each coupled rocking wall in the 2D model per floor. In the 2D model, the partition wall lengths were distributed between the three rocking wall panels.

5. Effects of partition walls on the response of mass timber building

Eight different variations of partition walls were considered: hospitality (Hsp) and apartment (Apt) partition wall densities, combined with four different partition wall types: fixed (F), slip track (ST), distributed gap (DG), and corner gap (CG). For both the 5-story and 12-story structures, the bare rocking wall structure model (no partition walls) and each partition wall variation model were subjected to eigenvalue analysis, pushover analysis, and time history analysis to assess the inclusion of partition walls in a mass timber building. The nonlinear analyses were solved with a Newton-Raphson algorithm and dynamic analyses employed a Newmark integrator with constant (average) acceleration across the time step.

5.1. Eigenvalue analysis

Using eigenvalue analysis, vibration periods of the first five modes

Table 3 Partition wall length.

Buildings		Apt.		Hsp.	Hsp.		
		Total	Coupled rocking wall	Total	Coupled rocking wall		
5-story	Partition Length (m)	276.5	69.1	138.3	34.6		
12-story	Partition Length (m)	347.6	43.5	173.8	21.7.		

were obtained. Table 4 shows the periods for the bare structures and the eight variations mentioned above. To facilitate the comparison, the percent change of the ith natural period of the structure ΔT_i is calculated to understand the change in dynamic properties when adding partition walls

$$\Delta T_i^n = \frac{(T_i^n - T_i^{bare})}{T_i^{bare}} \times 100 \tag{2}$$

where T_i^n is the ith mode period of the structure with the nth partition wall variation and T_i^{bare} is the ith mode period of the structure without partitiona walls. A negative ΔT_i indicates a decrease in the period. These period shifts are illustrated in Fig. 12.

By including partition walls, the periods of all modes and for all partition wall variations were observed to decrease due to the stiffening of the structure. The partition wall type influenced the modal periods more than partition wall density. The most significant period shift of about 30% was observed for the first mode of F-Apt in both buildings, and the effect of CG detailing was minor. Remarkably, in CG-Apt, the first mode periods of 5-story and 12-story buildings were reduced by only 2.2% and 2.5%, and the effect was even less in other modes. The period shifts for other partition details were somewhere in between these two extremes.

In all cases, the first mode period shift was the largest among all modes. Among all the partition walls, only the Fixed (F) detailing reduced the period by more than 20%, suggesting that using fixed detailing is likely to affect the response significantly. In similar studies for a concrete moment frame building [47], the period shift was limited to 8%. This comparison suggests the importance of including partition walls in the analysis of mass-timber buildings due to their inherent flexibility relative to concrete structures.

5.2. Nonlinear pushover analysis

Nonlinear static pushover analyses were performed to assess the shear capacities of buildings. This analysis provided an estimation of the force-deformation characteristics of the buildings and the relative contribution of the partition walls to stiffness and strength. Fig. 13 presents pushover curves of 5 story and 12 story buildings for all partition wall types and densities. The pushover curves are calculated for one coupled rocking wall unit. The results are presented as base shear coefficient V/W (i.e., lateral force V normalized by weight W collected by that wall unit) versus roof drift as a height percentage. In general, the pushover curves were tri-linearized into three specific regions: 1) initial stiffness (at the start of pushover analysis), 2) second stiffness (when lowest stiffness occurred), and 3) final stiffness (at the drift of 3%). Variations in stiffness and base shear coefficient were computed as follows:

Table 4 Periods of mode shapes.

$\Delta K_i = \frac{V_i}{K_{bare}} \times 100 \tag{3}$	$\Delta K_i = \frac{(K_i - K_{bare})}{K_{bare}} \times 100$	(3)
--	---	-----

$$\Delta\left(\frac{V}{W}\right)_{i} = \max\left(\left(\frac{V}{W}\right)_{i} - \left(\frac{V}{W}\right)_{bare}\right) \tag{4}$$

where K_i and $(\frac{V}{W})_i$ are the stiffness and base shear coefficient of the structure with partition walls and K_{bare} and $(\frac{V}{W})_{bare}$ are the stiffness and base shear coefficient of the structure with no partition walls. The stiffness variation (Eq. (3)) represents a percentage change and was applied to the initial stiffness $(\Delta K_1)_i$, second stiffness $(\Delta K_2)_i$, and final stiffness $(\Delta K_f)_i$. The variation in base shear coefficient (Equation (4)) represents an absolute change and was taken at the drift level that maximized building strength. These coefficients are tabulated for all buildings in Table 5.

For the 5-story building (Table 5), the initial stiffness increased by 2.6% for the CG-Hsp (negligible) to 113% for the F-Apt (more than doubled). Similar stiffness increases were seen for the 12-story building (3.1–13%). The second stiffness occurred in the mid-drift range where some parts of the coupled rocking wall, mainly UFPs, and all partition walls are yielded. In this region, the negative stiffness of partition walls, except CG, reduced the stiffness of the building. The final stiffness was relatively unaffected by partition walls, and only increased for Fixed detailing.

For the 5-story building, the maximum increase in base shear coefficient ranged from 0.028 for the CG-Hsp to 0.272 for the F-Apt. These maximums occurred between roof drifts of 0.39–0.89%, where the base shear coefficient of the bare structure was about 0.15. For the 12-story building, the maximum increase in base shear coefficient ranged from 0.002 (negligible) for the CG-Hsp density to 0.065 for the F-Apt, relative to the bare structure base shear coefficient of about 0.08 in the roof drift range (0.38–0.97%) where the maximums occurred. The maximum increase in base shear coefficient in both buildings occurred below 1% roof drift since partition walls yield at drifts well less than 1%. Each partition wall type has a negative stiffness region somewhere after yielding (see the backbone curves in Fig. 4), reducing its relative effect on the total base shear coefficient.

5.3. Nonlinear time history analysis

5.3.1. Ground motion selection

A subset of the ATC-62/FEMA P-695 FEMA [9] far-field ground motion suite was utilized in this study. Twelve components from the set of 22 far-field records (44 individual components) were selected. These selected records are listed in Table 6 according to their record number in PEER Ground Motion Database [29]. The far-field suite was chosen to avoid pulse effects that might add complexity to the interpretation of the results. Three different shaking intensities were considered: service-

			ST		F		DG		CG	
	Mode	Bare (sec)	Hsp. (sec)	Apt. (sec)	Hsp. (sec)	Apt. (sec)	Hsp. (sec)	Apt. (sec)	Hsp. (sec)	Apt. (sec)
5 story	1	0.91	0.84	0.79	0.74	0.65	0.86	0.81	0.90	0.89
	2	0.28	0.26	0.25	0.24	0.21	0.27	0.25	0.28	0.27
	3	0.15	0.15	0.14	0.14	0.12	0.15	0.14	0.15	0.15
	4	0.11	0.11	0.11	0.10	0.09	0.11	0.11	0.11	0.11
	5	0.10	0.09	0.09	0.09	0.08	0.09	0.09	0.10	0.10
12 story	1	2.15	1.96	1.81	1.71	1.48	2.00	1.87	2.12	2.10
-	2	0.62	0.58	0.55	0.52	0.47	0.59	0.56	0.61	0.61
	3	0.31	0.30	0.28	0.28	0.25	0.30	0.29	0.31	0.31
	4	0.20	0.19	0.19	0.18	0.17	0.20	0.19	0.2	0.20
	5	0.15	0.14	0.14	0.14	0.13	0.15	0.15	0.15	0.15

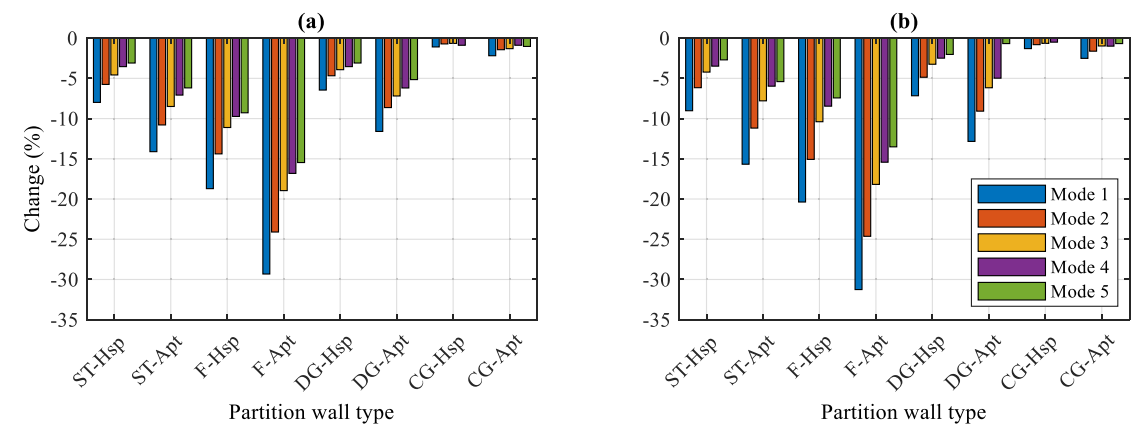


Fig. 12. Partition wall effect on periods (a) 5-story (b) 12-story.

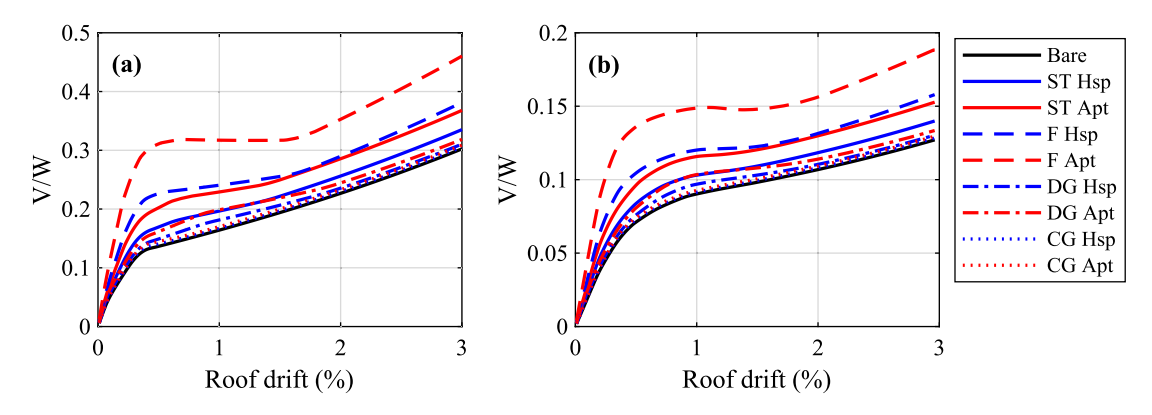


Fig. 13. Pushover curves of buildings including the partition walls (a) 5-story (b) 12-story.

Table 5Pushover statistics.

		Slip-Track		Fixed		Distributed Gap		Corner Gap	
		Hsp.	Apt.	Hsp.	Apt.	Hsp.	Apt.	Hsp.	Apt.
5-story	$(\Delta K_1)_i$	20.1	39.8	57.3	113	15.8	31.3	2.6	5.1
	$(\Delta K_2)_i$	-21.7	-43.3	-51.3	-102.6	-16.4	-32.7	-0.01	0.14
	$(\Delta K_f)_i$	4.0	8.3	20.0	40.2	-1.2	-2.2	-0.1	0.04
	$\Delta\left(\frac{V}{W}\right)_i$	0.04	0.07	0.09	0.18	0.02	0.05	0.004	0.009
12-story	$(\Delta K_1)_i$	23.9	47.3	67.8	133	18.8	37.1	3.1	6.1
	$(\Delta K_2)_i$	-33.3	-64.0	-81.1	-150	-22.0	-49.3	0.54	0.03
	$(\Delta K_f)_i$	6.1	12.5	29.2	58.4	-1.6	-2.8	0.01	0.20
	$\Delta\left(\frac{V}{W}\right)_i$	0.014	0.027	0.033	0.065	0.007	0.013	0.002	0.003

level earthquake (SLE) with a 72-year return period, design-basis earthquake (DBE) with a 475-year return period, and maximum considered earthquake (MCE) with a 2475 year return period. The motions were amplitude scaled for each intensity level so that the spectral acceleration of each motion corresponded to the target spectral acceleration at the bare structure fundamental period. The target spectra for DBE and MCE corresponded to ASCE 7-16 design spectra for site class D, and the target spectrum for SLE was calculated by the Unified Hazard Tool Tool [43]. Table 6 tabulates the selected earthquake record numbers, earthquake, station, PGAs, and scale factors for the MCE level. Fig. 14 shows scaled response spectra along with the target spectra for scaling for each intensity and building.

Nonlinear time history analysis was performed on the various 2D wall unit models using the above-ground motion suite scaled to the three

different intensities. The following responses were generated and analyzed: inter-story drift, story shear of the rocking wall units, and UFP forces.

5.3.2. Influence of partition walls on inter-story drift

Inter-story drift is one of the standard measurements for determining the performance of a structure during a seismic event. Design codes implement inter-story drift limits for immediate occupancy, life safety, and collapse prevention [2,10]. Fig. 15 compares representative roof drift (in %) of 5-story and 12-story buildings for the bare structure and F-Apt. Adding Fixed partition walls leads to roof drift reductions of 36% for the 5-story building and 17% for the 12-story building. In addition, higher frequency content can be seen in the drift history for the F-Apt due to its decreased fundamental period.

Table 6Ground motions selected from PEER [29].

No.	Record No.	Earthquake	Station Name	PGA (g)	SF-5 (MCE)	SF-12 (MCE)
1	125	Friuli	Tolmezzo	0.44	3.8	7.8
2	169	Imperial Valley	Delta	0.52	2.3	2.8
3	721	Superstition Hills	El Centro Imp. Co. Cent	0.82	2.4	2.5
4	752	Loma Prieta	Capitola	0.34	2.0	3.2
5	900	Landers	Yermo Fire Station	0.35	2.1	2.7
6	953	Northridge	Beverly Hills – 14145 Mulhol	0.51	0.8	2.0
7	1111	Kobe	Nishi-Akashi	0.36	2.1	2.3
8	1158	Kocaeli	Duzce	0.24	2.2	1.4
9	1244	Chi-Chi	CHY101	0.53	1.6	1.7
10	1602	Duzce	Bolu	0.51	1.2	1.7
11	1633	Manjil	Abbar	0.36	2.3	2.1
12	1787	Hector Mine	Hector	0.35	3.4	4.2

The peak inter-story drift was calculated in each story as the maximum difference in adjacent floor level displacement over time as a percentage of height. Fig. 16 shows the peak inter-story drift, averaged over the suite of motions, for both buildings and all three intensity levels.

For the SLE level, the inclusion of partition walls reduced the

maximum inter-story drift significantly. Peak inter-story drifts were most reduced for F-Apt, by maximum of 55% and 54% in any story for the 5-story and 12-story buildings, respectively, compared to the bare structure. Thus, although fixed detailing causes damage at low drifts, the added stiffness can significantly benefit the building response and design for the SLE level. The least reduction of peak inter-story drift in the SLE was observed for CG-Hsp; peak drift in any story was reduced by a maximum of 4.8% and 7.2% for the 5-story and 12-story buildings, respectively. Hence, if this detailing were to make its way into practice, the designer need not consider the effect of partition walls in the design and analysis of the buildings. The peak inter-story drifts of the other building types fell between these two extremes, and the only building type that realized inter-story drift reductions of more than 50% was F-Apt. Moreover, another conventional detailing, slip-track detailing, led to significant drift reductions. Peak drift reductions of up to 37% and 42% in the 5-story building and up to 26% and 31% in the 12-story building were observed for ST-Hsp and ST-Apt.

Peak inter-story drift reductions when considering the effects of partition walls were lower for DBE and MCE than for SLE intensity, but still significant. For example, for F-Apt subjected to DBE level, the peak inter-story ratios decreased by a maximum of 46% and 45% for the 5 and 12-story buildings, respectively. For F-Apt subjected to MCE level, the peak inter-story drift ratios decreased by 36% and 29% for the 5 and 12 story buildings, respectively. Moreover, the inclusion of partition walls changed the stiffness distribution, which resulted in a change in the drift profile in buildings. For example, in DBE and MCE levels, the maximum

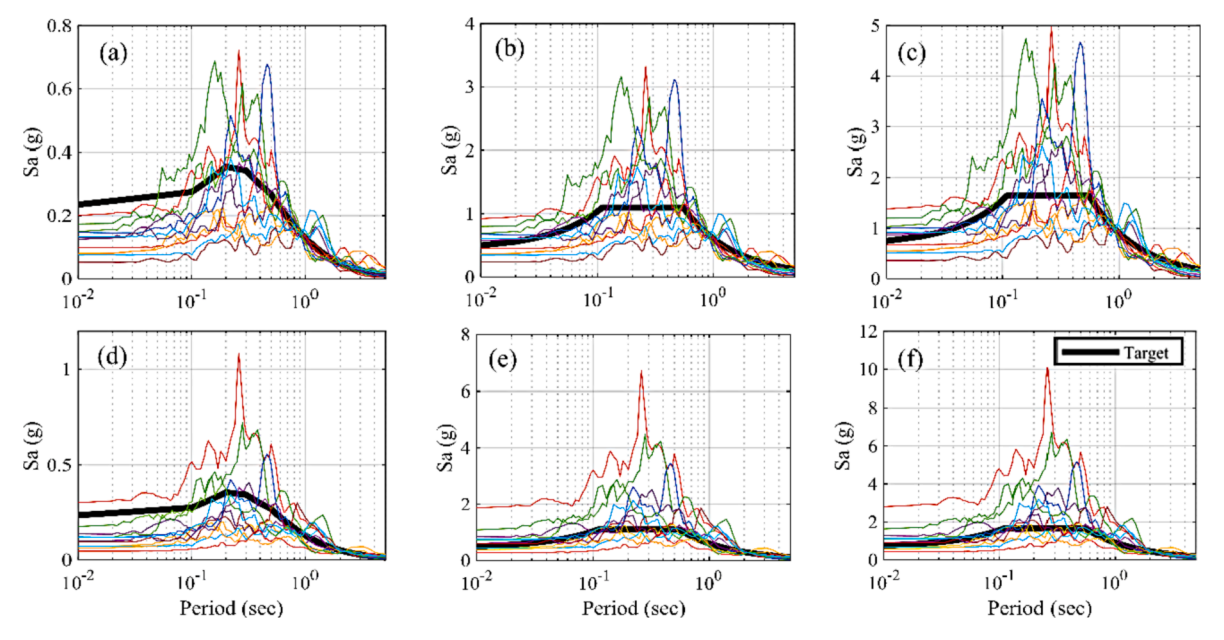


Fig. 14. Scaled response spectra (a) 5-story - SLE (b) 5-story - DBE (c) 5-story - MCE (d) 12-story SLE (e) 12-story - DBE (f) 12-story - MCE.

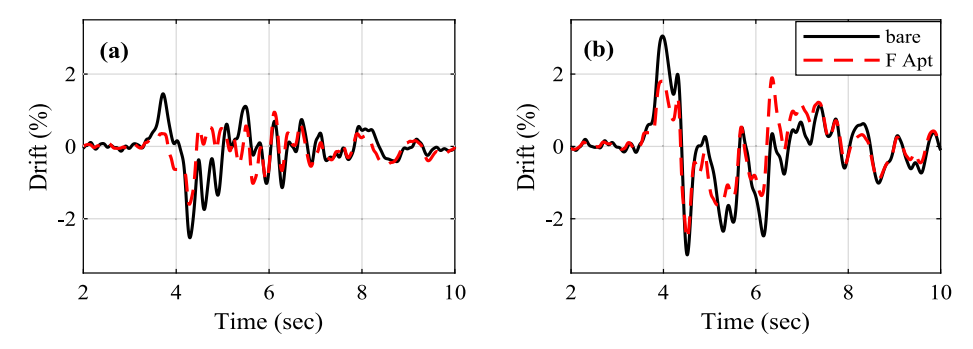


Fig. 15. Drift histories for GM 1- Friuli in MCE (a) 5 story (b) 12 story.

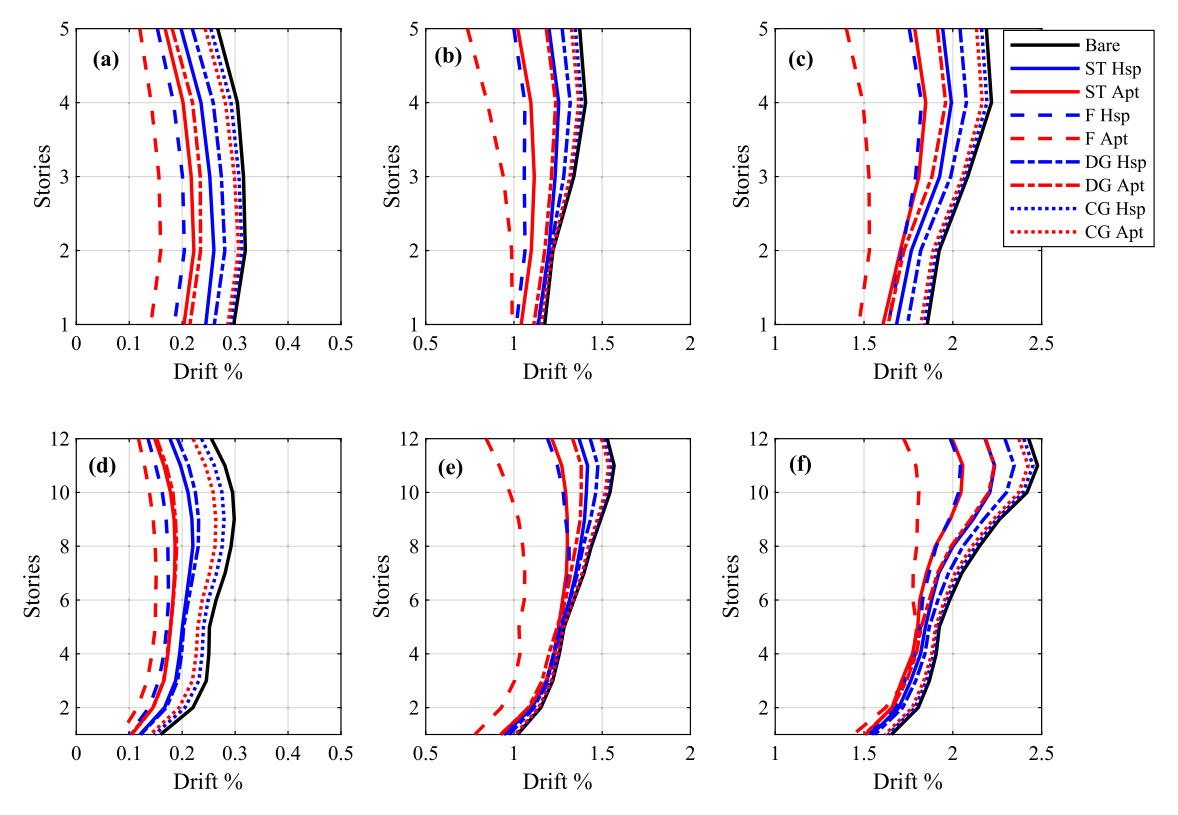


Fig. 16. Peak drift variation through the height (a) SLE-5 story (b) DBE-5 story (c) MCE-5 story (d) SLE-12 story (e) DBE-12 story (f) MCE-12 story.

inter-story drift reduction occurred in the upper stories where the peak story drift was observed.

For all building types/details, inter-story drift ratios remained below

the FEMA 356 limits [10], which are 0.7% for SLE, 2.5% for DBE, and 5% for MCE. However, these buildings were designed without considering the partition walls. In general, accounting for partition walls,

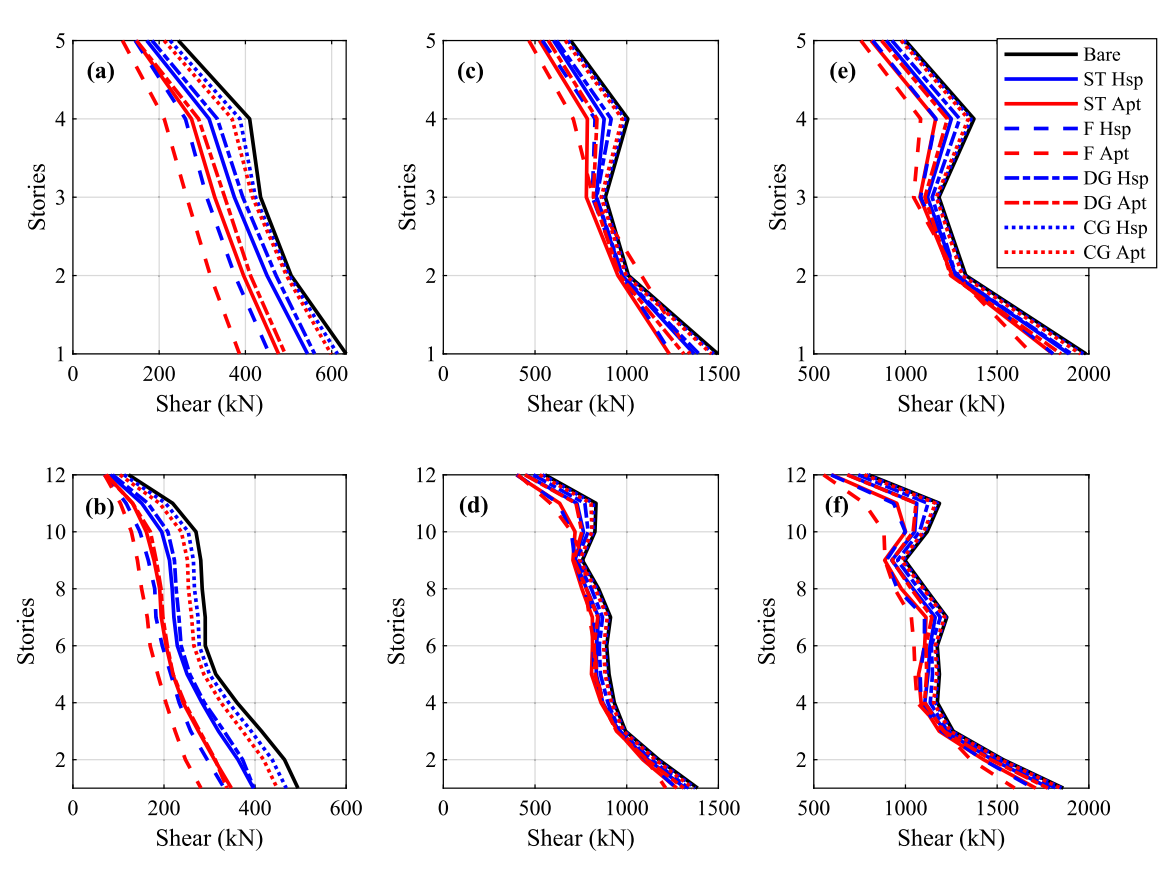


Fig. 17. Rocking wall shear variation through the height (a) SLE-5 story (b) SLE-12 story (c) DBE-5 story (d) DBE-12 story (e) MCE-5 story (f) MCE-12 story.

especially those with fixed details with considerable stiffness and strength, may benefit the design of the relatively flexible mass timber building with post-tensioned rocking walls either by reducing the building drift and helping to keep it under code limits or leading to a more economical design. On the other hand, partition walls detailed with corner gap (CG), for example, can be neglected in the building design due to their insignificant reduction in building drift, even though they help eliminate damage to the framing of partition walls [17].

5.3.3. Effects on story shear

Rocking wall story shear reflects the peak force demands and the governing lateral load on each story for design. The rocking wall story shear was calculated by summing the forces in the three rocking wall panel elements (UFP and PT forces were omitted). Fig. 17 shows the peak rocking wall story shear averaged over all the motions for each intensity level.

At all intensity levels, reductions in rocking wall story shears were observed for the buildings with partition walls relative to the bare structure due to story drift reductions. Rocking wall story shears decreased more for SLE than for DBE and MCE levels due to the high contribution of partition wall strength at lower drifts. SLE level rocking wall story shear reductions (maximum over all stories) ranged from 1% for CG-Hsp to 53% for F-Apt in the 5-story building. For the 12-story building, the rocking wall story shear reductions ranged from 4% for CG-Hsp to 52% for F-Apt.

For the DBE level, rocking wall story shear reductions for CG-Hsp (minimum over all building types) were 7% for the 5-story and 2% for the 12-story buildings. For F-Apt (maximum over all building types), story shear reductions were 32% and 30% for the 5-story and 12-story buildings, respectively. For the MCE level, partition walls reduced the

rocking wall story shears value by 24% and 35% for the 5-story and 12-story F-Apt building type, while story shear reductions for CG-Hsp were negligible.

Moreover, the rocking wall shear profile varied for different building types since partition walls changed the distribution of strength over the height of the rocking wall. For example, partition walls reduced the rocking wall shear more uniformly at the SLE than other intensity levels. For example, the story shear reduction for the 5-story F-Apt building varied over the height from 37% to 53%. This variation over height was 7% to 32% at the DBE level and 4% to 24% at the MCE level. In addition, the story shear tended to be most reduced at the base and the upper stories (Fig. 17 (c) and (e)).

6. Summary of results

Fig. 18 shows the average percent change of inter-story drift, rocking wall story shear, and summation of story UFP force for the structure with partition walls with respect to the bare structure. These values were computed by averaging the percent change of quantities with respect to the bare structure over the ground motions and then again over the stories, and provides a single measure for each building type.

As shown in Fig. 18, the inclusion of partition walls in the model affected the response of the building at the SLE level more considerably than other intensity levels. For example, assuming DG-Apt in a 5-story building reduced average inter-story drift by 28%, 9%, and 11% for SLE, DBE, and MCE, respectively. This trend was more significant for the UFP force than for other response parameters. For example, for the 12-story building, even CG-Apt resulted in a 14% reduction in UFP force at the SLE level, while it had a negligible effect at other intensity levels. This observation suggests that the UFP forces are post-yield at higher

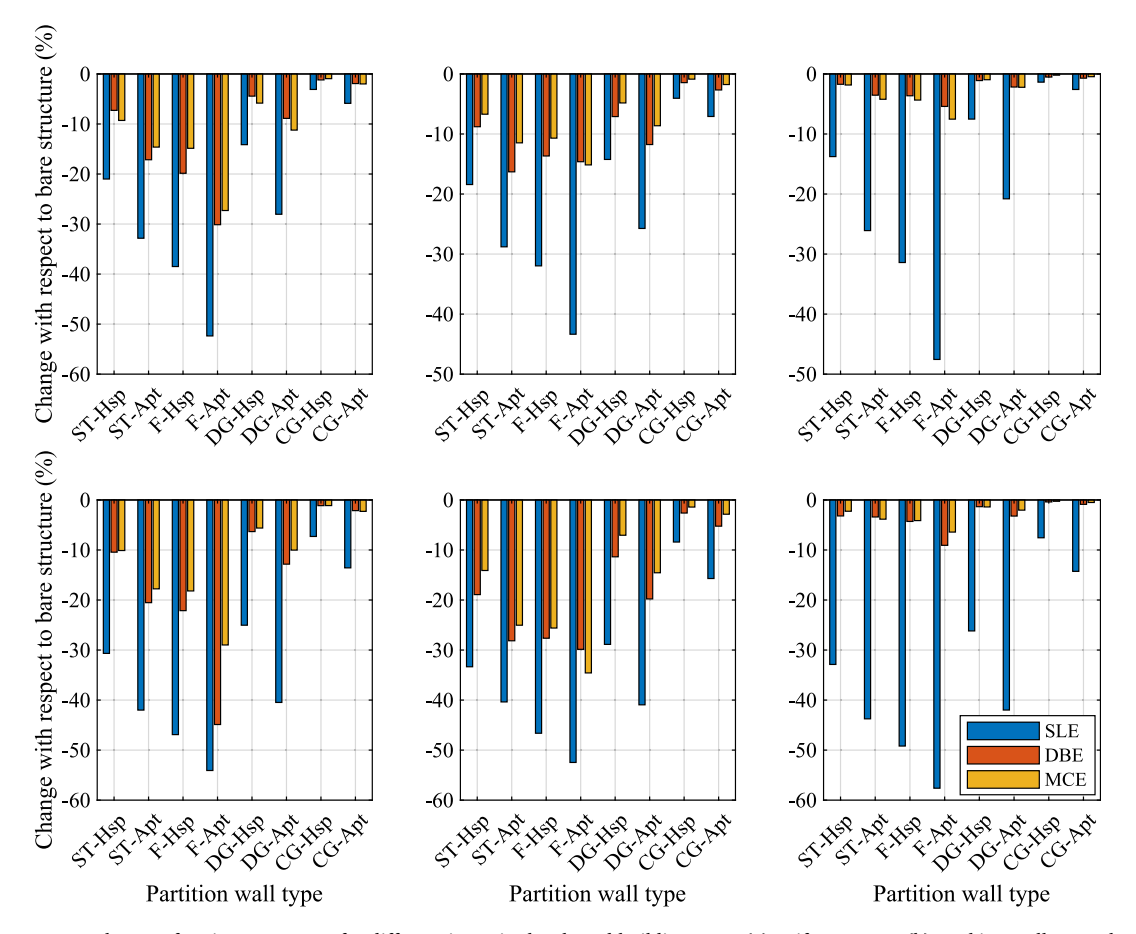


Fig. 18. Average percent change of various responses for different intensity levels and building types (a) Drift – 5-story (b) Rocking wall story shear – 5-story (c) UFP force – 5-story (d) Drift – 12-story (e) Rocking wall shear – 12-story (f) UFP force – 12-story.

intensity levels, and thus less sensitive to incremental changes in drift. In addition, the effect of partition wall stiffness on structural element forces was also more considerable at the SLE level than other intensity levels. For example, ST-Hsp reduced the average rocking wall story shear in the 5-story building by 18%, 9%, and 7% for the SLE, DBE, and MCE, respectively (Fig. 18(b)).

In summary, including strength and stiffness of partition walls in the building models has the benefit of reducing demands on the structure and corresponding design parameters in these buildings, especially for SLE intensity, which has a frequent return period of 50 years. SLE mainly assesses the serviceability of a structure, wherein little to no structural damage and only minor damage to nonstructural elements is allowed. Thus, the inclusion of partition wall stiffness will help the structure satisfy the SLE level targets. In particular, reducing forces in the UFPs to below yield (and preventing the need for UFP replacement at the SLE) is greatly beneficial. However, as the SLE is not the governing intensity for the design of structural elements, including partition walls for structural design is less critical.

7. Conclusion

This paper has addressed the effect of partition walls on the dynamic response of mass timber buildings with post-tensioned rocking wall lateral systems. A 2D numerical model of a coupled rocking wall unit was developed for buildings with two different heights (5-story and 12-story), and concentrated springs were added to the models to represent the effects of various densities and types of partition walls. Four different wall configuration details (fixed, slip track, slip track with distributed gap or DG, slip track with corner gap or CG) with two different densities (8 variations in total) were considered. Each model was evaluated using modal, pushover, and time-history analysis techniques. Moreover, time-history analyses were performed for three different earthquake intensities. Finally, different building response parameters were evaluated, and the significant findings are summarized as follows:

- From eigenvalue analysis, the vibration periods in all modes decreased relative to the bare structure due to the stiffening effect of the partition walls. The fundamental period decreased the most of all modal periods, with percentage decreases ranging from 1% to 29% and 1% to 31% for 5 and 12 story buildings, respectively.
- Partition walls affected the total stiffness of the wall unit over the entire drift range of pushover analysis, and caused significant increases in the initial stiffness and decreases in the stiffness after yielding.
- From dynamic analysis, including the partition walls in the model generally resulted in reductions of inter-story drift, rocking wall story shear, and UFP forces that were significant depending on the partition wall type and density. These reductions were more significant for the SLE level earthquake than for DBE or MCE. Since DBE or MCE generally controls design, the significance may not be apparent. However, the results of loss estimation studies, which generally predict that low-level events contribute significantly to life cycle costs, will be more affected by including partition walls in the models.
- Representing partition walls using simplified spring models was simple and effective in considering their effects in design and analysis. Omitting the effects of partition walls will lead to a more conservative building design.
- Among all the partition wall types, fixed connection detailing had the
 most effect on the structure. The fixed connection detailing stiffens
 the building, lowers drift demands, and lowers force demands in the
 rocking walls significantly as forces are carried both by structural
 elements and partition walls. On the other hand, CG walls had almost
 no influence on the stiffness and strength of buildings. Based on the
 results, the influence of partition walls can be omitted for the CG
 detail generally and for the slip track or DG detail in buildings with

lower density of partition walls. In other cases, including the effect of partition walls led to noteworthy reductions in drift and design forces, which would translate to a benefit in design.

Acknowledgments

This material is based upon work supported by the National Science Foundation under Grant No. CMMI-1635363. Any opinions, findings, conclusions, or recommendations expressed in this publication are those of the authors and do not necessarily reflect the views of the National Science Foundation.

Funding

This material is based upon work supported by the National Science Foundation under Grant No. CMMI-1635363. The authors are grateful for this support. Any opinions, findings, conclusions, or recommendations expressed in this publication are those of the authors and do not necessarily reflect the views of the National Science Foundation.

CRediT authorship contribution statement

Hamed Hasani: Conceptualization, Methodology, Software, Data curation, Writing – original draft, Visualization, Investigation. **Keri L. Ryan:** Supervision, Validation, Writing – review & editing, Project administration, Funding acquisition.

Declaration of Competing Interest

The authors declare that they have no known competing financial interests or personal relationships that could have appeared to influence the work reported in this paper.

References

- Araya-Letelier G, Miranda E, Deierlein G. Development and testing of a friction/ sliding connection to improve the seismic performance of gypsum partition walls. Earthq Spectra 2019;35(2):653–7. https://doi.org/10.1193/123117EQS270M.
- [2] ASCE. ASCE/SEI 7–16: Minimum design loads and associated criteria for buildings and other structures. Reston, Virginia, USA: The American Society of Civil Engineers; 2017.
- [3] Baird A, Smith T, Palermo A, Pampanin S. Experimental and numerical Study of U-shape Flexural Plate (UFP) dissipators. New Zealand Society for Earthquake Engineering (NZSEE) Annual Technical Conference, Wellington, New Zealand, 9; 2014.
- [4] Buchanan A, Deam B, Fragiacomo M, Pampanin S, Palermo A. Multi-story prestressed timber buildings in New Zealand. Struct Eng Int: J Int Assoc Bridge Struct Eng (IABSE) 2008;18(2):166–73. https://doi.org/10.2749/ 101686608784218635
- [5] Chancellor N, Eatherton M, Roke D, Akbaş T. Self-centering seismic lateral force resisting systems: High performance structures for the city of tomorrow. Buildings 2014;4(3):520–48. https://doi.org/10.3390/buildings4030520.
- [6] Davies RD, Retamales R, Mosqueda G, Filiatrault A. Experimental seismic evaluation, model parameterization, and effect of cold-formed steel-framed gypsum partition walls on the seismic performance of an essential facility; 2011.
- [7] Davies R, Retamales R, Mosqueda G, Filiatrault A. Seismic evaluation, parameterization, and effects of cold-formed steel framed gypsum partition walls. Technical Rep. MCEER-11-0005, State Univ. of New York, Buffalo, NY; 2011.
- [8] Di Cesare A, Ponzo FC, Lamarucciola N, Nigro D. Experimental seismic response of a resilient 3-storey post-tensioned timber framed building with dissipative braces. Bull Earthq Eng 2020;18(15):6825-48.
- [9] FEMA (Federal Emergency Management Agency). Quantification of building seismic performance factors. Washington, DC, USA; 2009.
- [10] FEMA. Prestandard and commentary for the seismic rehabilitation of buildings (FEMA 356). Washington, DC: Federal Emergency Management Agency; 2000.
- [11] FEMA (Federal Emergency Management Agency). Seismic performance assessment of buildings. Volume 2- Implementation Guide. FEMA P-58-2, 2, 365; 2012.
- [12] Filiatrault A, Uang C-M, Folz B, Christopoulos C, Gatto K. Reconnaissance Report of the February 28, 2001 Nisqually (Seattle-Olympia) Earthquake, Structural Systems Research Project Report No. SSRP-2000/15, University of California, San Diego, La Jolla, CA; 2001.
- [13] Fiorino L, Bucciero B, Landolfo R. Evaluation of seismic dynamic behaviour of drywall partitions, façades and ceilings through shake table testing. Eng Struct 2019;180:103–23.

- [14] Furley J, van de Lindt JW, Pei S, Wichman S, Hasani H, Berman JW, et al. Time-to-Functionality Fragilities for Performance Assessment of Buildings. J Struct Eng 2021;147(12). https://doi.org/10.1061/(ASCE)ST.1943-541X.0003195.
- [15] Ganey RS. Seismic design and testing of rocking cross laminated timber walls. The University of Washington (Doctoral dissertation); 2015.
- [16] Hasani H, Ryan K, Amer A, Ricles J, Sause R. Pre-test seismic evaluation of drywall partition walls integrated with a timber rocking wall. Proceedings of the 11th US National Conference on Earthquake Engineering. 2018.
- [17] Hasani H, Ryan KL. Experimental Cyclic Test of Reduced Damage Detailed Drywall Partition Walls Integrated with a Timber Rocking Wall. J Earthq Eng 2021. https://doi.org/10.1080/13632469.2020.1859005.
- [18] Lee T-H, Kato M, Matsumiya T, Suita K, Nakashima M. Seismic performance evaluation of nonstructural components: Drywall partitions. Earthq Eng Struct Dyn 2007;36(3):367–82. https://doi.org/10.1002/eqe.638.
- [19] Magliulo G, Petrone C, Capozzi V, Maddaloni G, Lopez P, Manfredi G. Seismic performance evaluation of plasterboard partitions via shake table tests. Bull Earthq Eng 2014;12(4):1657–77. https://doi.org/10.1007/s10518-013-9567-8.
- [20] Matsuoka Y, Suita K, Yamada S, Shimada Y, Akazawa M. Nonstructural component performance in 4-story frame tested to collapse. In: The 14th World Conference on Earthquake Engineering, 8. Beijing, China; 2008.
- [21] Mazzoni S, Mckenna F, Scott MH, Fenves GL. Open System for Earthquake Engineering Simulation (OpenSees) OpenSees Command Language Manual; 2007.
- [22] McCormick J, Matsuoka Y, Pan P, Nakashima M. Evaluation of nonstructural partition walls and suspended ceiling systems through a shake table study. In: Structures Congress 2008: Crossing the Borders; 2008. https://doi.org/10.1061/ 41016(314)223.
- [23] Miliziano A, Granello G, Palermo A, Pampanin S. Overview of connection detailing for post-tensioned dissipative timber frames. Struct Eng Int 2020;30(2):209–16.
- [24] Miranda E, Mosqueda G, Retamales R, Pekcan G. Performance of nonstructural components during the 27 February 2010 chile earthquake. Earthq Spectra 2012; 28(1 suppl1):453–71.
- [25] Mosqueda G. Interior cold-formed steel framed gypsum partition walls -Background document FEMA P-58/BD-3.9.32; 2016.
- [26] Motosaka M, Mitsuji K. Building damage during the 2011 off the Pacific coast of Tohoku Earthquake. Soils Found 2012;52(5):929–44.
- [27] Mulligan J, Sullivan TJ, Dhakal RP. Experimental seismic performance of partlysliding partition walls. J Earthq Eng 2020:1–26.
- [28] Pali T, Macillo V, Terracciano MT, Bucciero B, Fiorino L, Landolfo R. In-plane quasi-static cyclic tests of nonstructural lightweight steel drywall partitions for seismic performance evaluation. Earthq Eng Struct Dyn 2018;47(6):1566–88. https://doi.org/10.1002/eqe.3031.
- [29] PEER, PEER Ground Motion Database. Pacific Earthquake Engineering Research Center: 2021. https://ngawest2.berkeley.edu/ (Jun. 24, 2021).
- [30] Pei S, van de Lindt JW, Barbosa AR, Berman JW, McDonnell E, Daniel Dolan J, et al. Experimental seismic response of a resilient 2-story mass-timber building with post-tensioned rocking walls. J Struct Eng 2019;145(11):04019120. https://doi.org/10.1061/(ASCE)ST.1943-541X.0002382.
- [31] Ponzo FC, Di Cesare A, Lamarucciola N, Nigro D, Pampanin S. Modelling of post-tensioned timber-framed buildings with seismic rocking mechanism at the column-foundation connections. Int J Comput Methods Exp Measur 2017;5(6):966–78.

- [32] Ponzo FC, Di Cesare A, Lamarucciola N, Nigro D. Seismic design and testing of post-tensioned timber buildings with dissipative bracing systems. Front. Built Environ. 2019;5:104.
- [33] Reitherman R, Sabol T. Nonstructural Damage. In: John Hall (Ed.), Northridge Earthquake of January 17, 1994 Reconnaissance Report, Earthquake Spectra, Vol. 11, Supplement C, Earthquake Engineering Research Institute, Oakland, CA; 1995.
- [34] Retamales R, Davies R, Mosqueda G, Filiatrault A. Experimental seismic fragility of cold-formed steel framed gypsum partition walls. J Struct Eng 2013;139(8): 1285–93.
- [35] Rahmanishamsi E, Soroushian S, Maragakis E. "Manos", Sarraf Shirazi R. Analytical model to capture the in-plane and out-of-plane seismic behavior of nonstructural partition walls with returns. J Struct Eng,2017;143:04017033. https://doi.org/10.1061/(ASCE)ST.1943-541X.0001769.
- [36] Ryan K, Hasani H. Experimental Seismic Test of Drywall Partition Walls with Improved Detailing for Damage Reduction. 17th World Conference on Earthquake Engineering (17WCEE). 2020.
- [37] Shakeel S, Fiorino L, Landolfo R. Numerical modelling of lightweight steel drywall partitions for in-plane seismic performance evaluations. Ingegneria Sismica 2020; 37(1):64–83.
- [38] Soroushian S, Maragakis EM, Ryan KL, Sato E, Sasaki T, Okazaki T, et al. Seismic simulation of an integrated ceiling-partition wall-piping system at e-defense. II: evaluation of nonstructural damage and fragilities. 2016;142(2):1–17. https://doi. org/10.1061/(ASCE)ST.1943-541X.0001385.
- [39] Taghavi S, Miranda E. Response assessment of nonstructural building elements. Report PEER 2003/05, Pacific Earthquake Engineering Research Center, University of California, Berkeley, 96; 2003.
- [40] Tasligedik AS, Pampanin S, Palermo A. In-Plane cyclic testing of nonstructural drywalls infilled within RC frames. In: 15th World Conference on Earthquake Engineering (15WCEE), Lisbon, Portugal; 2012.
- [41] Tasligedik AS, Pampanin S, Palermo A. Low damage seismic solutions for nonstructural drywall partitions. Bull Earthq Eng 2013;13(4):1029–50.
- [42] Tasligedik AS, Pampanin S, Palermo A. Low damage seismic solutions for nonstructural drywall partitions. Bull Earthq Eng 2015;13(4):1029–50.
- [43] Unified Hazard Tool. (2021). https://earthquake.usgs.gov/hazards/interactive/ (Jun. 27, 2021).
- [44] Wang X, Pantoli E, Hutchinson TC, Restrepo JI, Wood RL, Hoehler MS, et al. Seismic performance of cold-formed steel wall systems in a full-scale building. J Struct Eng 2015;141(10):04015014. https://doi.org/10.1061/(ASCE)ST.1943-541X.0001245.
- [45] Whittaker AS, Soong TT. An overview of nonstructural components research at three U.S. earthquake engineering research centers. In: Proceedings of Seminar on Seismic Design, Performance, and Retrofit of Nonstructural Components in Critical Facilities, Applied Technology Council, ATC-29-2: 271-280, Redwood City, CA; 2002
- [46] Wilson AW. Numerical modeling and seismic performance of post-tensioned crosslaminated timber rocking wall systems. Washington State University (Master Thesis): 2018.
- [47] Wood RL, Hutchinson TC. A numerical model for capturing the in-plane seismic response of interior metal stud partition walls. Technical Report MCEER-12-0007; 2012.
- [48] Zhou Y, Li R, Lu XL. Earthquake-resilient tall buildings using rocking walls. In: 15th World Conference on Earthquake Engineering; 2012. p. 10.